Pergamon

Int. J. Heat Mass Transfer. Vol. 38, No. 17, pp. 3127–3134, 1995

0017–9310/95 $9.50+0.00

0017–9310(95)00098–4

Line-by-line calculations of the absorption of infrared radiation by water vapor in a box-shaped enclosure filled with humid air

GABRIEL N. SCHENKER and BRUNO KELLER

Institute of Building Technologies, Swiss Federal Institute of Technology, ETH-Hönggerberg, CH-8093 Zurich, Switzerland

(*Received* 23 *June* 1994 *and in final form* 17 *February* 1995)

Abstract—We have calculated the local absorption of thermal infrared radiation in humid air under non-equilibrium conditions: constant air temperature and humidity, contained in a room with a higher constant surface temperature ($\Delta T = 5$ K). The result shows a non-negligible heat transfer of 3–6 W m^{-3} K^{-1} from the surface to the air due to the absorption by the water vapor. The absorption is mainly concentrated to an air layer of 10–30 cm near to the wall. The interaction is very much increased near to corners and edges of the room.

1. INTRODUCTION

For the computation of the energy necessary for heating and/or cooling of rooms and also for the estimation of comfort, the thermal behavior of rooms is simulated with more or less complicated simulation programs (see, e.g. ref. [1]). Most of them treat the thermal coupling between the room boundaries (walls, floors, etc.), the air and the occupant in an engineering way: use of global coupling (or film) coefficients for thermal radiation and for convection; or precise calculation of the radiation field combined with a global coupling to the air volume, etc.

It has been shown by various authors [2, 3] that simulations performed with many of these programs using the same configuration still result in big differences. This is most probably due to the over-simplification of the thermal coupling mechanisms in a room. For these reasons, much more sophisticated programs have recently been developed for the computation of the flow fields in a room under specific conditions (see, e.g. ref. [4]). Most of them are based on finite volume methods and they neglect any coupling to the radiation field. They are quite successful for the simulation of flow fields due to momentum ventilation, where the momentum of the incoming air dominates. For the displacement ventilation and/or natural ventilation, however, thermal buoyancy plays an important role, and thermal coupling to the room boundaries becomes the key factor. This coupling requires a detailed knowledge of the transitions in the boundary layers. Up to now this interaction has been taken into account by means of convective turbulent boundary layer models alone (k–ε models [5]).

The air flow field and the room boundaries are subject to three principal interactions:

(1) direct boundary layer convective coupling as a local coupling;

(2) indirect interaction with the radiation field through the temperature distribution on the surfaces: long-range radiation coupling, partially bypassing the convective coupling;

(3) direct interaction with the radiation field through the absorption and re-emission of infrared radiation by the water vapor in the air (relative humidity 30–60%): short-range radiation coupling.

All three interactions can principally influence the flow field. The first and the third affect the direct heat transfer and therefore the film coefficients. The second one influences the temperature distribution.

Apart from the purely air flow oriented models, only a few papers have dealt with the long-range coupling through the radiation field (e.g. refs. [6–10]). These studies have already shown that the radiation field in fact does play an important role even at room temperature [10].

Even fewer papers have dealt with the interaction through absorption and emission by the water vapor content of the air (e.g. refs. [11–14]); because of the mathematical complexity, different simplifications [15–17] have been used: instead of detailed high resolution spectra, band approximations have been used; the influence of temperature and pressure variations on the spectra has been neglected; and the geometry has been mostly reduced to a simple two-dimensional or even one-dimensional situation, neglecting corners and edges with significantly higher radiation interaction and being of importance for the starting conditions of boundary layers.

Whereas wide-band (or statistical) models are accurate enough for strongly absorbing media, narrow-band or even line-by-line calculations (e.g. the absorp-

NOMENCLATURE

a	absorption coefficient
A	surface area
$\mathrm{d}^l Q$	lth order differential of the quantity Q
e	emissive power
i	radiation intensity
L	mean beam length
M	number of areas the surface of the enclosure is composed of
N	number of spectral lines
q	energy flux
Q	energy per unit time
r	radial coordinate
R	radius of ring
s	at distance s
S	spectral line intensity
T	temperature
V	volume
x, y, z	Cartesian coordinates.

Greek symbols

α	absorptance
γ	half width at half maximum of spectral line
ε	emissivity or total emittance
θ	angle from normal of area
ν	wavenumber
ξ	orthogonal distance from area
τ	transmittance
χ	specific absorption
ω	solid angle.

Subscripts

a	absorbed
b	black body
c	corrected
e	emitted
g	of the gas
i	ith spectral line
j	jth surface area
r	radiation
v	water vapor
w	of the wall
ν	wavenumber dependent
0	initial value.

Superscripts

$'$	directional value.

tion and emission of each spectral line of water vapor has to be calculated individually) have to be used for optically thin media [18]. Results from such wide-band calculations show that, in fact, for low water vapor contents, the overall emissivity of the air volume is not greatly changed [16, 19, 20]; but these calculations cannot describe or quantify local interactions, e.g. within a boundary layer.

For these reasons we shall determine in detail the interaction between the thermal radiation field and the humid air in a realistic three-dimensional box-shaped geometry on the basis of high resolution water vapor spectra [21]. We work with an air volume of constant temperature enclosed in a box of constant but different temperature. This simplified situation is chosen to set the effect of the infrared absorption of the water vapor apart, avoiding any interference with the effects of temperature gradients in the gas. These effects, as for example the naturally evolving convection currents or the thermal boundary layer, would mask the effect we are looking for and would complicate the problem. The situation with temperature gradients will be investigated in a subsequent publication.

2. ANALYSIS

Figure 1 shows the absorption spectra of water vapor at a temperature of $T_0 = 296$ K in combination with the characteristic radiation intensity of an object at $T = 20°C$ considered to radiate like a black body, e.g. the walls of the enclosure or the fluid. It is clear at once that for typical room temperatures only the absorption lines in the range 0–500 cm^{-1} and the lines constituting the 1595 cm^{-1} absorption band are important. The rotational bands of H_2O at 3755, 5331 and 7250 cm^{-1}, which play an important role in combustion processes, can be completely neglected in our model.

The model used for this study is illustrated by Fig. 2. Boundary conditions are of the first kind, i.e. the three-dimensional box-shaped enclosure is surrounded by isothermal walls. The basic assumptions made in the analysis are as follows:

(1) the enclosed air is at a given uniform temperature and stagnant;
(2) All physical properties are constant (i.e. independent of temperature);
(3) the walls are gray diffuse emitters and reflectors of radiation;
(4) the density of the radiatively participating fluid (air–water vapor mixture) is uniform.

The validity of the first assumption can be questioned for the high precision calculations which we perform. A non-uniform temperature profile (e.g. refs. [22, 23]) near the wall, however, would significantly increase the complexity of the computations [see equation (4) below] and consequently seriously augment the necessary CPU times. For a more detailed discussion on this subject refer to Section 1.

The assumption of constant (temperature–independent) physical properties is primarily a numerical

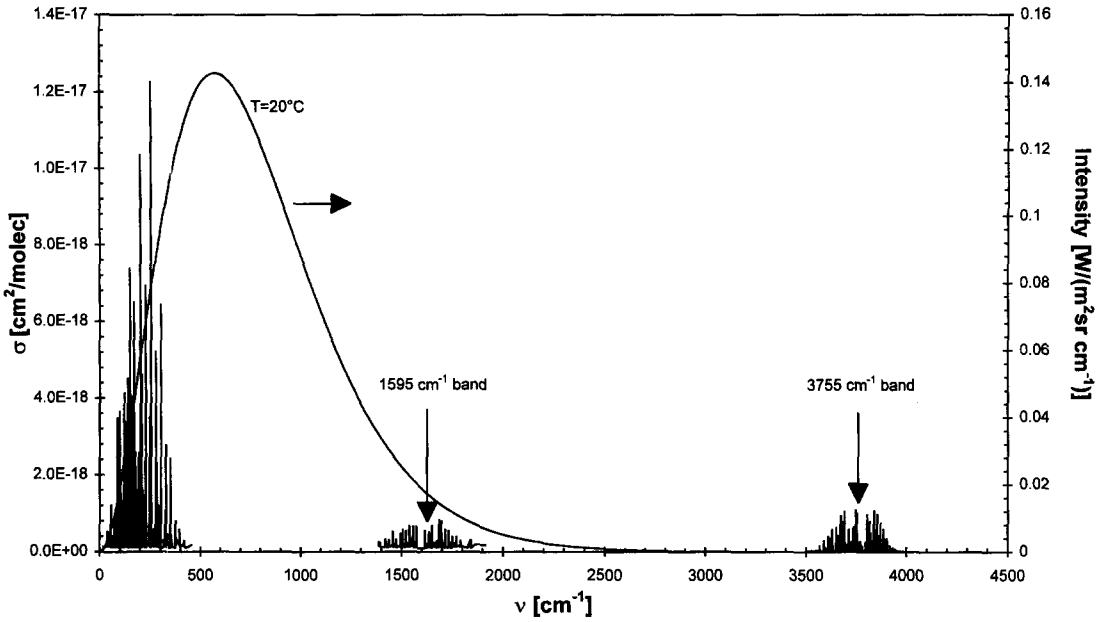

Fig. 1. Absorption spectra of water vapor combined with the spectral intensity of a black body at a temperature of $T_b = 20°C$.

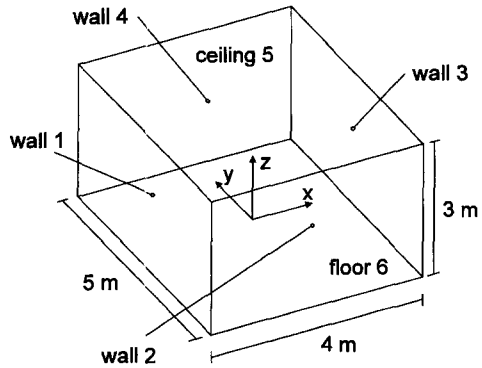

Fig. 2. Isothermal box shaped enclosure filled with an air–water vapor mixture.

convenience and is almost always adopted in analyses in order to decrease the number of independent parameters.

Toor and Viskanta [24] have shown that for most enclosures the assumption of gray diffuse walls is a reasonable approximation to reality.

The shape of a single line of the absorption spectrum of water vapor is assumed to be Lorentzian. Furthermore, the gas is assumed to be in a state of local thermodynamic equilibrium.

The spectral absorption coefficient for the Lorentz (dispersion) line shape is

$$a_{v,i}(s) = \frac{S_i(s)}{\pi} \cdot \frac{\gamma_i(s)}{(v-v_i)^2+\gamma_i^2(s)} \tag{1}$$

where s is the spatial position, $S_i(s)$ is the line strength of line i and $\gamma_i(s)$ is the half width at half maximum (HWHM) of the line. The reference of the spectral position is the line center v_i. $S_i(s)$ is assumed to be a function of temperature $T(s)$ only, whereas $\gamma_i(c(s),p(s))$ may be a function of the concentration (molar fraction) of active gas $c(s)$, total gas pressure $p(s)$ and temperature.

We compute the absorption spectrum of H_2O as a superposition of all Lorentzian-shaped spectral lines in the spectral region of interest (i.e. 0–2500 cm^{-1})

$$a_v(s) = \sum_{i=1}^{N} a_{v,i}(s) = \sum_{i=1}^{N}\left[\frac{S_i(s)}{\pi} \cdot \frac{\gamma_i(s)}{(v-v_i)^2+\gamma_i^2(s)}\right]. \tag{2}$$

Here $N = 5950$ is the number of spectral lines found in the wavenumber interval mentioned above. For an absorbing and emitting but non-scattering medium the equation of radiative transfer is given by [19]

$$(\mathbf{s}\cdot\nabla)\cdot i'_v = -a_v(i'_v - i'_{vb}(T_g)) \tag{3}$$

where s is the direction of propagation. The first term on the right-hand side of the above equation gives the decrease of intensity due to absorption in the medium under consideration and the second term derives from the increase of intensity due to the emission of the same medium. Integrating the above equation from a reference position $s' = 0$ cm to $s' = s$ results in

$$i'_v(s) = i'_v(0)e^{-\int_0^s a_v\,ds'} + \int_0^s a_v \cdot i'_{vb}(T_g(s')) \cdot e^{-\int_{s'}^s a_v\,ds''}\,ds' \tag{4}$$

where the first term on the right-hand side is now the contribution due to boundary radiation (i.e. walls) and the second term stems from the emission and reabsorption of radiation by the medium. If the tem-

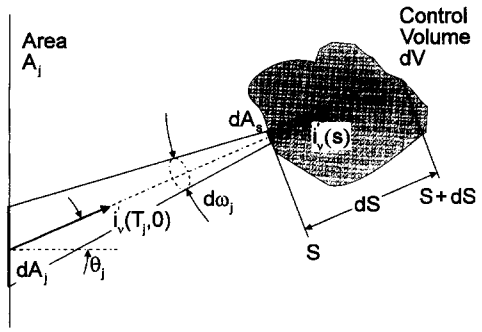

Fig. 3. Geometry for the derivation of the absorption through a volume of medium.

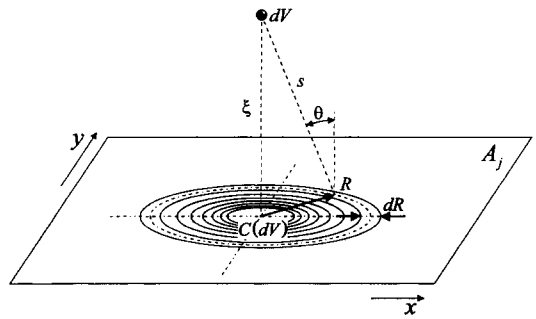

Fig. 4. Subdivision of the rectangular area into rings of radius R and variable thickness dR.

perature T_g and the absorbtivity a_v are considered constant throughout the fluid (i.e. for an isothermal and homogeneous fluid), equation (4) reduces to

$$i'_v(s) = i'_v(0)e^{-a_v s} + i'_{vb}(T_g)(1-e^{-a_v s}). \quad (5)$$

If we now consider an infinitesimal control volume dV of the participating fluid inside the enclosure as in Fig. 3, with absorption coefficient $a_v(v,T,p)$ within dV, the change of intensity in dV as a result of absorption is [19]

$$di'_v(s) = -i'_v(s)a_v ds. \quad (6)$$

The radiative power absorbed in the differential subvolume $ds\,dA_s$ of the control volume dV per frequency interval and per unit solid angle from this incident radiation is

$$d^5Q'_{v,a} = -di'_v dA_s dv d\omega_j = i'_{v,j}(s)a_v ds dA_s dv d\omega_j \quad (7)$$

where the solid angle $d\omega_j$ spanned by the surface element dA_j is defined as

$$d\omega_j = \frac{dA_j \cos(\theta_j)}{s^2} \quad (8)$$

and dA_s is the projected area normal to $i'_{v,j}$. The notation $d^5Q'_{v,a}$ has been chosen in analogy to ref. [19]. We have put the index j to clarify that the intensity i'_v originates from the surface element dA_j. The energy coming from the direction of dA_j and absorbed by all of dV is found by integrating over dV (note that dV is regarded as a second order differential $dA \cdot ds$),

$$d^4Q'_{v,a} = i'_{v,j}(s)a_v dv d\omega_j \int_{dV} dA_s ds = a_v i'_{v,j}(s) dV dv d\omega_j. \quad (9)$$

In order to obtain the contribution of the whole enclosure, it is necessary to integrate over all $d\omega_j$ of surface j and take the sum over all surfaces A_j enclosing the fluid

$$d^3Q_{v,a} = \sum_{j=1}^{N} a_v dV dv \int_{A_j} i'_{v,j}(s) d\omega_j. \quad (10)$$

If we further consider that the walls are gray emitters and reflectors, then the intensity of the radiation emitted by the wall is $i'_{v,j} = \varepsilon_j i'_{vb,j}$ and the emissive power [19] $e_{vb,j} = \pi i'_{vb,j}$. By also setting the transmissivity $\tau_v(s) = e^{-a_v s}$, we then have the following relation for the absorbed energy.

$$d^3Q_{v,a} = \frac{a_v dV dv}{\pi} \sum_{j=1}^{N} \left[\int_{A_j} [\varepsilon_j e_{vb,j}(T_j)\tau_v(s) + e_{vb,g}(T_g)(1-\tau_v(s))] \cdot \frac{\cos\theta_j dA_j}{s^2} \right]. \quad (11)$$

To account for the radial symmetry of the integral (Fig. 4), we can modify the integral part of equation (11) as follows

$$2\pi \cdot \int_0^{r_{j,max}} K(r)[\varepsilon_j e_{vb,j}(T_j)\tau_v(s) + e_{vb,g}(T_g)(1-\tau_v(s))] \cdot \frac{\xi_j r_j \cdot dr_j}{s^3} \quad (12)$$

where $K(r) \leqslant 1$ accounts for rings which do not entirely fit into area A_j, and ξ_j is the orthogonal distance from the control volume dV to the surface element A_j. The exact formula for $K(r)$ will be deduced in the following section.

The gas contained in the control volume dV also emits energy. It can be shown that the following relation holds [19]:

$$d^3Q_{v,e} = 4a_v e_{vb}(T_g) dV dv. \quad (13)$$

Finally, the net heat gain or loss of the control volume dV is found by integrating over the whole spectral range of interest

$$d^2Q = \int_{v_{min}}^{v_{max}} (d^3Q_{v,a} - d^3Q_{v,e}) dv. \quad (14)$$

In the literature d^2Q is also called div q_r or net heat gain through radiation and has as units watts per cubic meter. For our simplified set-up with constant temperatures in the gas and on the walls we can define a specific absorption χ as long as $(T_w - T_g)/T_w \ll 1$ by

$$\chi = \frac{d^2Q}{\Delta T} = \frac{\text{div}\, q_r}{\Delta T} \tag{15}$$

where $\Delta T = T_w - T_g$. This value allows us to make comparisons with other transfer mechanisms.

3. METHOD OF SOLUTION

Computations are performed to investigate interactions of infrared radiation and water vapor in a box-shaped enclosure by employing the mathematical model described in the previous section.

Air at a reference pressure of 1 atm, temperature $T_g = 293$ K and relative humidity $f_{rel} = 50\%$ is the considered medium. The wall temperatures are set to $T_w = 298$ K and their emissivities to $\varepsilon_w = 1$.

First, the absorption spectrum of water vapor is computed at a spectral resolution of $d\nu = 0.01\ cm^{-1}$. The resolution is then reduced to $d\nu = 0.1\ cm^{-1}$ by a smoothing algorithm in order to reduce computer run time. Since the mean distance from spectral line to spectral line is of the order of $0.42\ cm^{-1}$, this reduction in resolution does not overlap lines but only affects their shape. Test calculations with high ($d\nu = 0.01\ cm^{-1}$) and lower ($d\nu = 0.1\ cm^{-1}$) resolution showed no significant differences in the result (of the order of 1%).

The necessary line information is given by the HITRAN database [21], with which we calculated the line intensities S_i, the air broadened halfwidths γ_i, and the spectral positions of the lines ν_i for the standard situation ($T = 296$ K, $p = 1$ atm). The line intensities are accurate to $\sim 5\%$ for the stronger lines. For weaker lines, the uncertainty is $\approx 20\%$. In general, the accuracy of the line positions is better than $\Delta\nu = \pm 0.005\ cm^{-1}$.

Secondly, the inner surface of the enclosure is subdivided into M rectangular areas A_j. The integral [equation (12)] is solved by means of a finite differencing algorithm. Therefore each area A_j is subdivided into a set of rings (Fig. 4) with radius R_k and thickness dR_k, where $k \in \{0,1,\ldots,k_{max}\}$. The thickness of the rings increases with increasing distance from the center $C_j(dV)$, i.e.

$$dR_k = f \cdot dR_{k-1} \quad f > 1 \tag{16}$$

to account for their increasing distance from the control volume dV and thus the reduced solid angle they subtend. With equation (16) the value for k_{max} is given by

$$k_{max} = \frac{\ln(1+(f-1)\cdot R_{max})}{\ln(f)} - 1. \tag{17}$$

$C_j(d\nu)$, in turn, represents the orthogonal projection of the center of mass of the control volume dV onto the plane in which area A_j lies. The starting value of the thickness of the rings is chosen as follows:

$$dR_0 = \min\left(dR_{min}; \frac{\xi_j}{n}\right). \tag{18}$$

Rings that do not completely fit into area A_j are accounted for by the multiplication factor $K(r)$ [cf. equation (12)], which in turn is obtained by the following considerations. Here we suppose that C_j lies inside the considered area A_j but the case where this is not true can easily be solved in an analogous way. Let Δ_i, $i = 1,\ldots,4$ be the orthogonal distances of C_j from the borders of the area A_j. Then for $K(r)$ we have the following rules:

$$K(r) = \begin{cases} 0 & \text{if } r > R_{max} \\ 1 & \text{if } r \leqslant R_{min} \\ 1 - \sum_{i=1}^{4} \left[\frac{2\beta_i}{2\pi}\eta_i + \frac{\frac{\pi}{2} - \beta_i}{2\pi}\zeta_i \right] & \text{otherwise} \end{cases} \tag{19}$$

where

$$\cos(\beta_i) = \frac{\Delta_i}{r}; \quad R_{max} = \max_{\substack{i,j \in \{1,2,3,4\} \\ i \neq j}} [\sqrt{(\Delta_i^2 + \Delta_j^2)}] \tag{20}$$

$$R_{min} = \min_{i \in \{1,2,3,4\}} (\Delta_i)$$

and

$$\eta_i = \begin{cases} 1 & \text{if the ring intersects border } i \\ & \quad \text{of surface } Aj \text{ at least once} \\ 0 & \text{otherwise} \end{cases}$$

$$\zeta i = \begin{cases} 1 & \text{if the ring intersects border } i \\ & \quad \text{of surface } Aj \text{ exactly once} \\ 0 & \text{otherwise.} \end{cases} \tag{21}$$

The finite thickness of the rings can be neglected in the determination of $K(r)$ since $R_k \gg dR_k$ for every k.

In our simulations we chose $M = 6$, i.e. each wall, floor and ceiling represents an individual area A_j. A difference of less than 1% in the results was detected in varying the factor f between $f = 1.001$ and $f = 1.01$. Finally we performed our calculations with $dR_{min} = 0.02$ cm and $n = 50$. Equation (12) is solved for each infinitesimal spectral interval $d\nu$ in the range of interest and then integrated [equation (14)]. The whole process is repeated for every other control volume inside the enclosure.

Calculations have been performed on a network of several SUN SPARC 10 workstations at the Institute of Theoretical Physics at the Federal Institute of Technology in Zurich, Switzerland. The typical CPU time to compute $\text{div}(q_r)$ for one control volume dV is approximately 30 min.

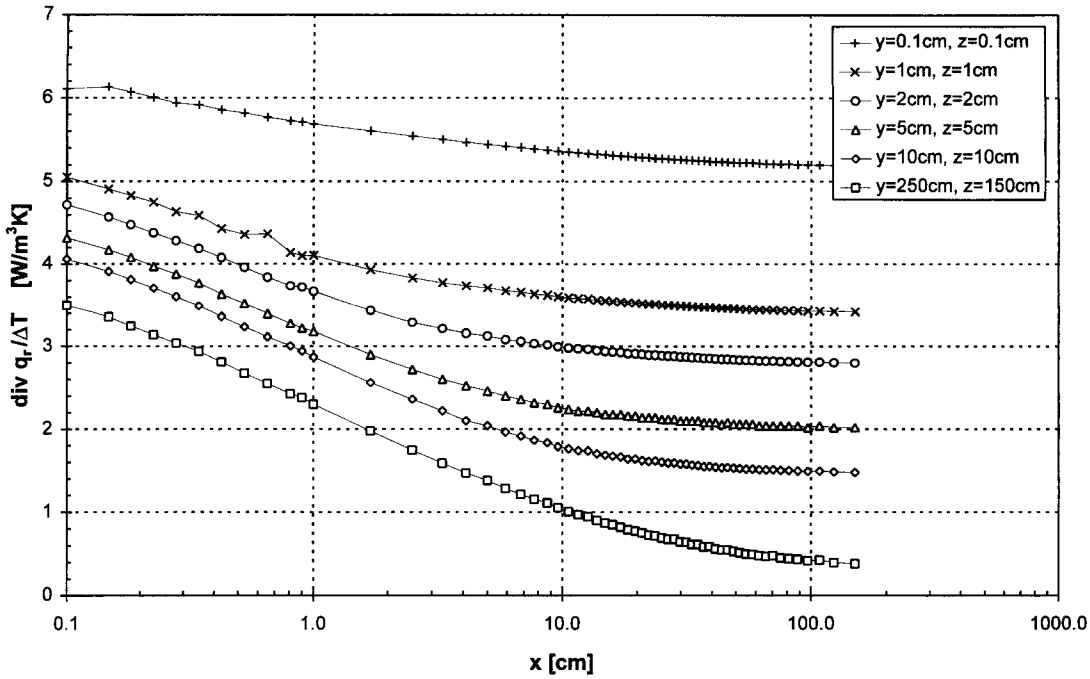

Fig. 5. Local specific heat absorption due to radiation as a function of the wall distance for air temperature $T_g = 293$ K, wall temperatures $T_w = 298$ K and relative humidity $f_{rel} = 50\%$.

4. RESULTS AND DISCUSSION

Figure 5 shows the net specific absorption,

$$\chi = \frac{div(q)}{\Delta T},$$

as a function of the distance to one wall for different locations within the box (Fig. 2). In spite of the low temperature, there exists a considerable specific absorption between 3 and 6 W m^{-3} K^{-1}. The specific absorption decreases exponentially within the first 10–30 cm of the air and flattens out to values between 0.4 and 3 W m^{-3} K^{-1}. This air layer of the first 10–30 cm from the wall corresponds approximately to the boundary layer which occurs under ambient conditions in natural convection in a room. In other words, under such conditions the absorption interaction would take place mainly in the boundary layers and would influence their temperature profile. This is in good agreement with the results of Benjelloun *et al.* [11] in other situations. It can be understood, by inspecting the water vapor spectra (Fig. 1), that the absorptance is mainly concentrated in narrow but deep lines.

Contrary to conclusions from low resolution spectra (well-dispersed absorptance), this leads to high local absorption coefficients which make the corresponding part of thermal radiation partially disappear after a short way in the air; because this 'cleaned away' part is small and will also be successively filled up by the contributions of deeper air layers, the overall emissivity of air volume will be changed only slightly by the absorption due to its humidity content [16, 19]. The concentration of the absorption of this small part of radiation power into a relatively thin air layer near to the wall, however, will have a non-negligible effect and influence the heat transition or the thermal coupling to the surface.

Integrating the specific absorption over the whole volume of the room considered yields the total absorbed power by the water vapor. By means of numerical integration we obtain:

$$Q = \int\int\int_V \operatorname{div} q_r \, dV = 263.9 \, [\mathrm{W}]. \qquad (22)$$

Due to the limited number of calculated reference points available and the linear interpolation algorithm we have adapted, this result represents a slightly too high value but certainly lies within the correct order of magnitude.

For a comparison with the other thermal transition mechanisms as convection or radiation, we should derive the corresponding film or transition coefficient. This, however, is not easy, as we now do not have a further local surface-to-surface (wall surface to 'surface' of air volume) interaction as in convection, but a surface-to-volume interaction. Each element of the volume has radiation absorbed from all surface elements of the room. We can deduce a corresponding transition coefficient α_v in the sense of a mean value if we make use of our set-up: constant wall temperatures and constant air temperature:

$$\alpha_v = \frac{Q}{(T_w - T_g) \cdot \sum A_i} = 0.56 \, [\mathrm{W\,m^{-2}\,K^{-1}}]. \qquad (23)$$

This value can be compared with the values for natural convection $\alpha_{nc} \approx 2\ W\ m^{-2}\ K^{-1}$ and thermal radiation $\alpha_{th} \approx 5 W\ m^{-2}\ K^{-1}$ (all in ordinary rooms under ambient conditions). Although it seems to be relatively small, it cannot be neglected.

This clearly demonstrates that the radiative coupling must be taken into account as soon as one deals with humid air under conditions of natural convection. In other words: the local heat transition between the wall surface and the air has to be completed by a non-negligible thermal radiation part and this part is a function of the humidity content of the air and of the radiation geometry (plane, edge, corner). Along edges and in corners, where the convective transition is very weak, the radiation part is strong, thus yielding soon a radiative dominance. To compare our computation with well-known results from the literature [16, 19, 25], we take the approximate method from Siegel and Howell [19]. With this method, the total radiation from the entire gas volume to all of the boundary can be determined. A heat balance between the gas and the emitting boundary of the enclosure is given by

$$\frac{Q_g}{A} = -\frac{Q_w}{A} = \sigma \cdot [\varepsilon_g(T_g) T_g^4 - \alpha_g(T_w) T_w^4] \quad (24)$$

where ε_g is the total emittance of the gas and α_g the total absorptance of the gas for radiation emitted from the wall at temperature T_w. Since in our model $\Delta T = (T_w - T_g) \ll T_w$ it follows that $\alpha_g \approx \varepsilon_g$ and therefore the above equation reduces to

$$\frac{Q_g}{A} = -\frac{Q_w}{A} = \sigma \cdot \varepsilon_g \cdot [T_g^4 - T_w^4]. \quad (25)$$

For our situation the mean beam length L for the limit of an optically thin gas is [19]

$$L = \frac{4V}{A} = 2.55 \cdot D \quad (26)$$

and for an optically thick gas the 'corrected' mean beam length L_c can be approximated by

$$L_c = 0.9 \cdot L. \quad (27)$$

With these values and the partial pressure of water vapor in our model, ε_g can be determined from experimental data [25]. We obtain a value of $\varepsilon_g \approx 0.12$ and thence

$$\tilde{\alpha}_v = \frac{Q_g}{A \cdot (T_w - T_g)} = 0.68\ [W\ m^{-2}\ K^{-1}]. \quad (28)$$

This must be compared with our result of $\alpha_v = 0.56\ W\ m^{-2}\ K^{-1}$ and confirms at least the order of magnitude.

5. CONCLUSIONS

Our results agree with the global considerations of gas radiation in an enclosure found in the literature. In addition, they demonstrate that:

(1) the heat transfer due to the radiation absorption in the water vapor content of the air is not negligible;

(2) the main part of the absorptance of water vapor is concentrated into a relatively thin layer near the wall surface—this is due to the narrow but deep absorption lines;

(3) there exists a pronounced dependency on the geometry, i.e. a strong increase of the absorptance near edges and corners.

Since this thin air layer approximately corresponds to the thickness of boundary layers in rooms with natural convection under ambient conditions, we conclude that the absorptance due to the water vapor will influence the temperature and possibly also the velocity profile in the boundary layers. Therefore a dependence of the convective heat transition on the humidity content of the air can be expected.

The pronounced interaction between infrared radiation and humidity near edges and corners opens new perspectives in the understanding of the conditions of surface condensation in rooms.

An experimental set-up is being developed to verify these calculations under controlled conditions. For this purpose, new heat flux sensors of ultra-high sensitivity have been developed at our Institute [26].

Acknowledgements—The authors wish to thank E. Heeb and A. Schönenberger of the Institute of Theoretical Physics at the Federal Institute of Technology in Zurich for their generosity concerning access to their computer network and for their useful advice regarding implementation problems of the program developed for this work.

REFERENCES

1. *Reference Manual* (2.1*A*): *How to Use DOE-2, Version* 2.1*A*, Lawrence Berkeley Laboratories, National Technical Information Service, Springfield (1994).
2. D. P. Bloomfield, The work of international energy agency Annex 21 on calculation of energy and environmental performance of buildings, *Proceedings of the Second BEPAC Conference*, pp. 59–66, York. David Bartholomew Associates, Reading (1994).
3. K. J. Lomas, Thermal program validation: the current status, *Proceedings of the Second BEPAC Conference*, pp. 73–82, York. David Bartholomew Associates, Reading (1994).
4. J. Ludwig, H. Qin and B. Spalding, *The PHOENICS Reference Manual, Rev.* 08, *SW Version* 1.5.1, CHAM Report No. TR/200 (1989).
5. J. Hinze, *Turbulence* (2nd Edn). McGraw-Hill, New York (1975).
6. M. Engelman and M.-A. Jamnia, Grey-body surface radiation coupled with conduction and convection for general geometries, *Int. J. Numer. Meth. Fluids* **13**, 1029–1053 (1991).
7. D. M. Kim and R. Viskanta, Effect of wall conduction and radiation on natural convection in a rectangular cavity, *Numer. Heat Transfer* **7**, 449–470 (1984).
8. Y. Li and L. Fuchs, A two-band radiation model for calculating room wall surface temperature. In *Recent Advances in Heat Transfer*, pp. 388–400. Elsevier, Amsterdam (1992).
9. Y. Li, L. Fuchs and M. Sandberg, Numerical prediction of airflow and heat-radiation interaction in a room with

displacement ventilation, *Energy Buildings* **20,** 27–43 (1993).
10. M. Behnia, J. A. Reizes and G. de Vahl Davis, Combined radiation and natural convection in a rectangular cavity with a transparent wall and containing a non-participating fluid, *Int. J. Numer. Meth. Fluids* **10,** 305–325 (1990).
11. Y. Benjelloun, M. Cherkaoui, J. L. Dufresne, R. Fournier, J. Y. Grandpeix and D. Palenzuela, Influence of infrared radiation on high Rayleigh number natural convection in cavities, *Eurotherm Seminar* No. 21, pp. 293–301 (1992).
12. T. Fusegi, K. Ishii, B. Farouk and K. Kuwahara, Natural convection–radiation interactions in a cube filled with a nongray gas, *Numer. Heat Transfer, A,* **19,** 207–217 (1991).
13. M. Cherkaoui, J. L. Dufresne, R. Fournier, J. Y. Grandpeix, A. Lahellec and D. Palenzuela, Two procedures for radiative calculation with narrow-band statistical model in a volume of gas at room temperature, *Eurotherm Seminar* No. 21, pp. 119–128 (1992).
14. A. Draoui, C. Beghein and F. Allard, Radiative couplings between the walls and a semi-transparent fluid enclosed in a two dimensional thermally driven cavity, *Eurotherm Seminar* No. 21, pp. 129–138 (1992).
15. R. M. Goody and Y. L. Yung, *Atmospheric Radiation* (2nd Edn), Chap. 4, pp. 125–188. Oxford University Press, New York (1989).
16. H. C. Hottel and A. F. Sarofim, *Radiative Transfer*, Chap. 6, pp. 211–217. McGraw-Hill, New York (1967).
17. J. M. Hartmann, R. Levi di Leon and J. Taine, Line by line and narrow-band statistical model calculations for H_2O, *J. Quant. Spectrosc. Radiat. Transfer* **32,** 119–127 (1984).
18. A. Soufiani, J. M. Hartmann and J. Taine, *J. Quant. Spectrosc. Radiat. Transfer* **33,** 243–257 (1985).
19. R. Siegel and J. R. Howell, *Thermal Radiation Heat Transfer* (3rd Edn). Hemisphere, Washington, DC (1992).
20. A. Huber, Wechselwirkung von Strahlung und Konvektion in Räumen, Internal Publication. LES, Swiss Federal Institute of Technology (1990).
21. L. S. Rothman, R. R. Gamache, A. Goldman, L. R. Brown, R. A. Toth, H. M. Pickett, R. L. Poynter, J.-M. Flaud, C. Camy-Peyret, A. Barbe, N. Husson, C. P. Rinsland and M. A. H. Smith, The HITRAN database: 1986 edition, *Appl. Opt.* **26,** 4058–4097 (1987).
22. E. Schmidt and W. Beckmann, Das Temperatur- und Geschwindigkeitsfeld von einer wärmeabgebenden senkrechten Platte bei natürlicher Konvektion, *Technd. Mech. Thermodyn.* **1,** 341–349; 391–406 (1930).
23. S. Ostrach, An analysis of laminar free convection flow and heat transfer about a flat plate parallel to the direction of the generating body force, National Advisory Committee for aeronautics, Technical report, p. 1111 (1953).
24. J. S. Toor and R. Viskanta, A critical examination of the validity of simplified models for radiant heat transfer analysis, *Int. J. Heat Mass Transfer* **15,** 1553 (1972).
25. H. C. Hottel, *Heat Transmission* (3rd Edn) (Edited by W. H. McAdams), Chap. 4. McGraw-Hill, New York (1954).
26. V. M. Meyer and B. Keller, A new supersensitive heat-flux sensor, *Proceeding of the Fifth Symposium Temperature and Thermal Measurement in Industry and Science*, Prague. TEMPMEKO '93 (1993).